Future projections of record-breaking sea surface temperature and cyanobacteria bloom events in the Baltic Sea

H. E. Markus Meier ⓘ, Christian Dieterich ⓘ, Kari Eilola,
Matthias Gröger, Anders Höglund, Hagen Radtke, Sofia Saraiva,
Iréne Wåhlström ⓘ

Abstract Aiming to inform both marine management and the public, coupled environmental-climate scenario simulations for the future Baltic Sea are analyzed. The projections are performed under two greenhouse gas concentration scenarios (medium and high-end) and three nutrient load scenarios spanning the range of plausible socio-economic pathways. Assuming an optimistic scenario with perfect implementation of the Baltic Sea Action Plan (BSAP), the projections suggest that the achievement of Good Environmental Status will take at least a few more decades. However, for the perception of the attractiveness of beach recreational sites, extreme events such as tropical nights, record-breaking sea surface temperature (SST), and cyanobacteria blooms may be more important than mean ecosystem indicators. Our projections suggest that the incidence of record-breaking summer SSTs will increase significantly. Under the BSAP, record-breaking cyanobacteria blooms will no longer occur in the future, but may reappear at the end of the century in a business-as-usual nutrient load scenario.

Keywords Climate change · Coastal seas · Cyanobacteria · Extremes · Numerical modeling · Sea surface temperature

INTRODUCTION

The Baltic Sea is a semi-enclosed, shallow sea with limited water exchange with the adjacent North Sea in northern Europe. The Baltic Sea catchment area is large compared to its sea surface (Fig. S1, Electronic supplementary

material), and increased population and intensified agriculture throughout the catchment have led to excessive river-borne nutrient loads since the 1950s causing the world's largest anthropogenic-induced hypoxic sea bottoms (e.g., Carstensen et al. 2014; Meier et al. 2019a, b). Consequently, environmental pressures such as eutrophication, input of hazardous substances, benthic habitat degradation, overfishing, and invasive species, together with changing climate, are intensively discussed (HELCOM 2018). As the physical conditions of the Baltic Sea, such as the long residence time and the pressure of the large population in the catchment area, are not unique compared to other coastal seas (e.g., Rabalais et al. 2010), the Baltic Sea, given the large amount of observations that have been collected, can serve as a study site and laboratory for many large marine ecosystems worldwide (Sherman et al. 2005).

To manage the marine ecosystem of coastal seas, future projections are of utmost importance (e.g., Meier et al. 2011a). Based on scenario simulations, nutrient load abatement strategies were adopted by all Baltic Sea neighboring countries facilitated by the Helsinki Commission (HELCOM), i.e., the so-called Baltic Sea Action Plan, BSAP (HELCOM 2013a). Based on agreed baseline values of ecosystem indicators, Good Environmental Status (GES) is supposed to be reached in 2021. These ecosystem indicators are observable quantities such as water clarity, e.g., measured by Secchi disk depth (henceforth called Secchi depth), and oxygen debt, i.e., the summer mean oxygen deficit due to biogeochemical oxygen consumption compared to saturated oxygen conditions (HELCOM 2013b; see Tables 1 and 2, last columns of the upper tables).

However, most recent assessments (HELCOM 2018) suggest that the present environmental status is not

Table 1 Modeled Secchi depth (in m) averaged over each sub-basin from Fig. 1 for the four scenario simulations under RCP 4.5. The upper and lower tables are for the historical (1976–2005) and future (2068–2097) periods, respectively. The ensemble mean and in the lower table also the future change (in %) relative to the historical period are shown. In the upper table, the reported status for 1970–2000 (Savchuk et al. 2006) and for 2007–2011 (HELCOM 2013b) and the envisaged Good Environmental Status (GES) (HELCOM 2013b) are added. The targets for the indicators Secchi depth and oxygen debt (Table 2) were calculated from historical observations. Exceeding the 95% confidence interval of the 'natural' variation of the indicator means during the pre-eutrophication period (1900–1940) is defined as a significant deviation from a relatively unaffected environmental status. For the other sub-basins either the baseline values of GES are not available or are not reached during the simulation period

1976–2005 Annual average		A	B	C	D	Ensemble mean	Obs[a]	Obs[b]	GES[b]
Basin number	Basin	Secchi depth (m)							
2	Kattegat	6.37	6.45	6.59	6.47	6.47	4.5	6.60	7.52
3	Öresund	6.54	6.59	6.68	6.50	6.58	7.0	7.19	6.33
4	Belt Sea	7.16	7.16	7.24	7.16	7.18	7.0	7.19	6.33
5	Arkona	7.31	7.36	7.46	7.13	7.31	7.8	8.20	7.36
6	Bornholm	7.28	7.35	7.43	7.13	7.30	7.8	7.93	8.05
7	E Gotland	7.50	7.61	7.60	7.44	7.54	7.8	7.43	8.78
8	NW Gotland	8.09	8.21	8.20	8.02	8.13	7.8	7.43	8.78
9	Gulf of Riga	4.65	4.67	4.71	4.73	4.69	3.0	3.30	3.90
10	Gulf of Finland	4.98	5.02	5.01	4.92	4.98	4.2	3.73	5.41
11	Archipelago Sea	5.18	5.32	5.24	5.24	5.25	–	–	–
12	Åland Sea	5.97	5.98	5.98	5.93	5.96	–	–	–
13	Bothnian Sea	6.13	6.14	6.16	6.12	6.14	6.0	4.95	6.89
14	Bothnian Bay	5.70	5.68	5.77	5.67	5.71	5.5	4.70	6.39
2068–2097 Annual average		A	B	C	D	Ensemble Mean			Mean change
Basin number	Basin	Secchi depth (m)							Secchi depth (%)
2	Kattegat	6.70	6.78	6.92	6.78	6.79			5.0
3	Öresund	7.29	7.33	7.15	7.25	7.25			10.3
4	Belt Sea	7.67	7.69	7.43	7.65	7.61			6.0
5	**Arkona**	**8.33**	**8.33**	**8.11**	**8.25**	**8.25**			**12.9**
6	**Bornholm**	**8.29**	**8.32**	**8.25**	**8.25**	**8.28**			**13.4**
7	E Gotland	8.53	8.59	8.63	8.54	8.57			13.7
8	**NW Gotland**	**8.83**	**8.83**	**9.10**	**8.83**	**8.90**			**9.4**
9	Gulf of Riga	5.16	5.10	5.23	5.12	5.15			9.9
10	**Gulf of Finland**	**5.44**	**5.40**	**5.62**	**5.39**	**5.46**			**9.7**
11	Archipelago Sea	5.94	5.91	6.27	5.87	6.00			14.3
12	Åland Sea	6.37	6.31	6.56	6.29	6.38			7.0
13	Bothnian Sea	6.42	6.38	6.57	6.35	6.43			4.8
14	Bothnian Bay	5.82	5.80	5.85	5.79	5.82			1.9

Sub-basins for which the baseline values of the GES will be achieved at the end of the century are marked in bold

[a]Savchuk et al. (2006), [b]HELCOM (2013b)

consistent with GES and many ecosystem components indicate a status which is 'not good'. Due to the memory in the system regarding the interlinked changes (such as the release of nutrients from sediments once the oxygen budget changes), the prospect of reaching GES overall by 2021 is unlikely, and full implementation of existing policy agreements and identification of new effective measures are clearly required. In this study, we contribute to this discussion by answering the question 'When will GES be reached ?', taking existing scenario simulations of future

climate (Saraiva et al. 2019), and their uncertainties, into account.

One motivation for reaching GES is the high recreational value of the Baltic Sea for the public. Tourism is an important economic sector in the region (HELCOM 2018). Indicators of environmental and ecological condition that affect cultural ecosystem services related to tourism include water temperature, water clarity, cyanobacteria blooms, macro algae onshore, biodiversity, etc. These indicators differ from the ecosystem indicators for GES.
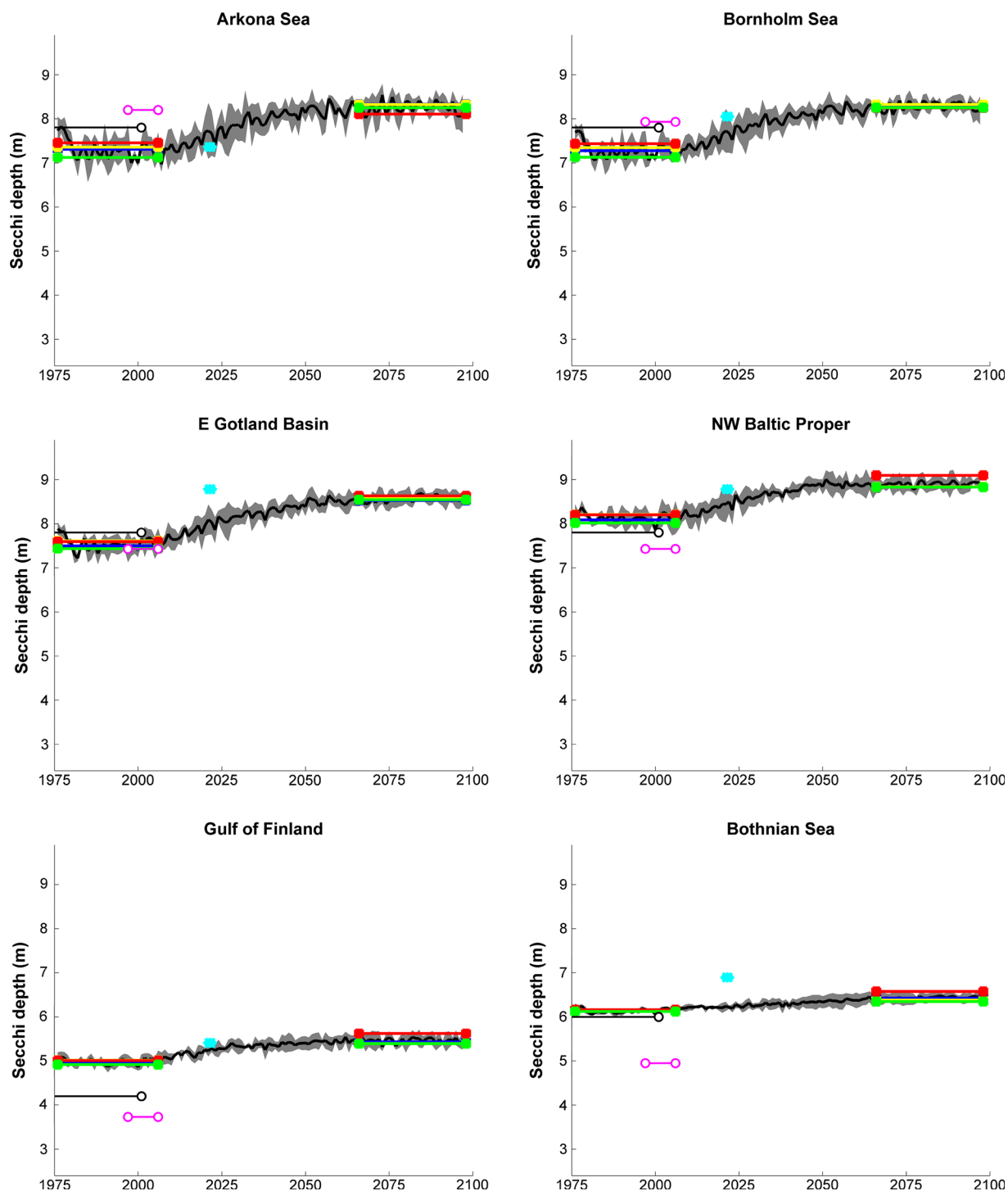
Fig. 1 Ensemble mean, annual average Secchi depth (in m) for 1976–2097 for selected sub-basins (black line) for BSAP and RCP 4.5. The gray shaded area denotes the range of ± 1 SD among the four ensemble members. The colored lines with solid squares at the beginning and end of the records are the averages for each climate simulation for the periods 1976–2005 and 2068–2097 (Model A—blue, Model B—yellow, Model C—red, Model D—green). The cyan dots are the HELCOM (2013b) thresholds for BSAP's Good Environmental Status (GES) shown in the year 2021 which is the year in which GES is supposed to be attained. The purple line with open circles is the mean (1997–2006) Secchi depth status from HELCOM (HELCOM 2013b; Table 4.3). The black line with the open circle is the median (1970–2000) Secchi depth from Savchuk et al. (2006; Table 3). The Savchuk values shown for the East Gotland Basin, the North-West Baltic Proper, Bornholm Basin, and Arkona Basin are those reported for the Baltic Proper. For further details see Table 1

Table 2 As Table 1 but for oxygen debt (in mg L^{-1}) averaged over each sub-basin from Fig. 2. In the upper table, the reported current status for 2007–2011 (HELCOM 2013b) and the envisaged Good Environmental Status (GES) (HELCOM 2013b) are added

1976–2005 Annual average		A	B	C	D	Ensemble mean	Obs[a]	GES[a]
Basin number	Basin	Oxygen debt (mg L^{-1})						
2	Kattegat	1.80	1.61	1.66	1.64	1.68	–	> 2
3	Öresund	2.63	2.24	2.39	2.36	2.40	–	> 2
4	Belt Sea	3.91	3.38	3.61	3.60	3.63	–	> 2
5	Arkona	2.72	2.34	2.33	2.78	2.54	–	–
6	Bornholm	6.76	7.12	6.83	7.32	7.01	7.10	6.37
7	E Gotland	10.45	10.06	10.17	10.28	10.24	10.54	8.66
8	NW Gotland	12.02	11.33	11.40	11.94	11.67	10.54	8.66
9	Gulf of Riga	0.84	0.69	0.60	0.78	0.73	–	–
10	Gulf of Finland	9.83	8.92	7.62	10.07	9.11	10.54	8.66
11	Archipelago Sea	0.05	0.03	0.04	0.06	0.04	–	–
12	Åland Sea	1.93	1.80	1.74	1.73	1.80	–	–
13	Bothnian Sea	2.39	2.09	2.08	2.15	2.18	–	–
14	Bothnian Bay	0.32	0.29	0.23	0.22	0.26	–	–
2068–2097 Annual average		A	B	C	D	Ensemble mean	Mean change	
Basin number	Basin	Oxygen debt (mg L^{-1})					Oxygen debt (%)	
2	Kattegat	1.47	1.44	1.33	1.41	1.41	− 16	
3	Öresund	2.14	2.00	1.94	1.95	2.01	− 16	
4	Belt Sea	3.30	3.07	3.54	3.07	3.25	− 10	
5	Arkona	1.81	1.75	2.13	1.79	1.87	− 26	
6	**Bornholm**	**4.73**	**4.79**	**5.57**	**4.60**	**4.92**	**− 30**	
7	**E Gotland**	**6.57**	**6.56**	**7.27**	**6.33**	**6.68**	**− 35**	
8	**NW Gotland**	**8.06**	**7.89**	**7.89**	**7.45**	**7.82**	**− 33**	
9	Gulf of Riga	0.20	0.19	0.05	0.18	0.16	− 79	
10	**Gulf of Finland**	**6.68**	**6.60**	**4.29**	**6.12**	**5.92**	**− 35**	
11	Archipelago Sea	0.03	0.02	0.02	0.02	0.03	− 42	
12	Åland Sea	0.97	1.28	0.71	1.33	1.07	− 40	
13	Bothnian Sea	1.25	1.58	0.59	1.65	1.27	− 42	
14	Bothnian Bay	0.05	0.20	0.02	0.16	0.11	− 59	

Sub-basins for which the baseline values of the GES will be achieved at the end of the century are marked in bold

[a] HELCOM (2013b)

Warm and clear water will attract tourists and recreationalists, whereas near-shore, harmful, and smelly algae mats or onshore macro algae will deter tourism.

Furthermore, indicators of the marine environmental status are commonly based on mean conditions. However, the perception of the recreational value of a beach site might be dominated by extreme events rather than by mean status, for example by the occurrence of extremely warm days. Hence, assessment of the changing occurrence of extreme events may be as important for the non-market benefits derived from aquatic environments as is assessment of mean environmental status.

As some of the indicators are not yet included in climate model simulations, such as macro algae onshore and biodiversity (e.g., Meier et al. 2011a; Saraiva et al. 2019), and because changes in extremes in the marine environment have not been addressed before, new challenges arise for scenario simulations and their analysis. One exception (disregarding all literature on projected sea-level extremes) is the Baltic Sea study by Neumann et al. (2012) who found

(1) an increasing probability that sea surface temperatures (SSTs) at the end of the century will exceed 18 °C in summer (June–August) in all Baltic sub-basins favoring cyanobacteria blooms;

(2) that future occurrence of hypoxic conditions ($O_2 < 2$ mL L^{-1}) in the near-bottom water will
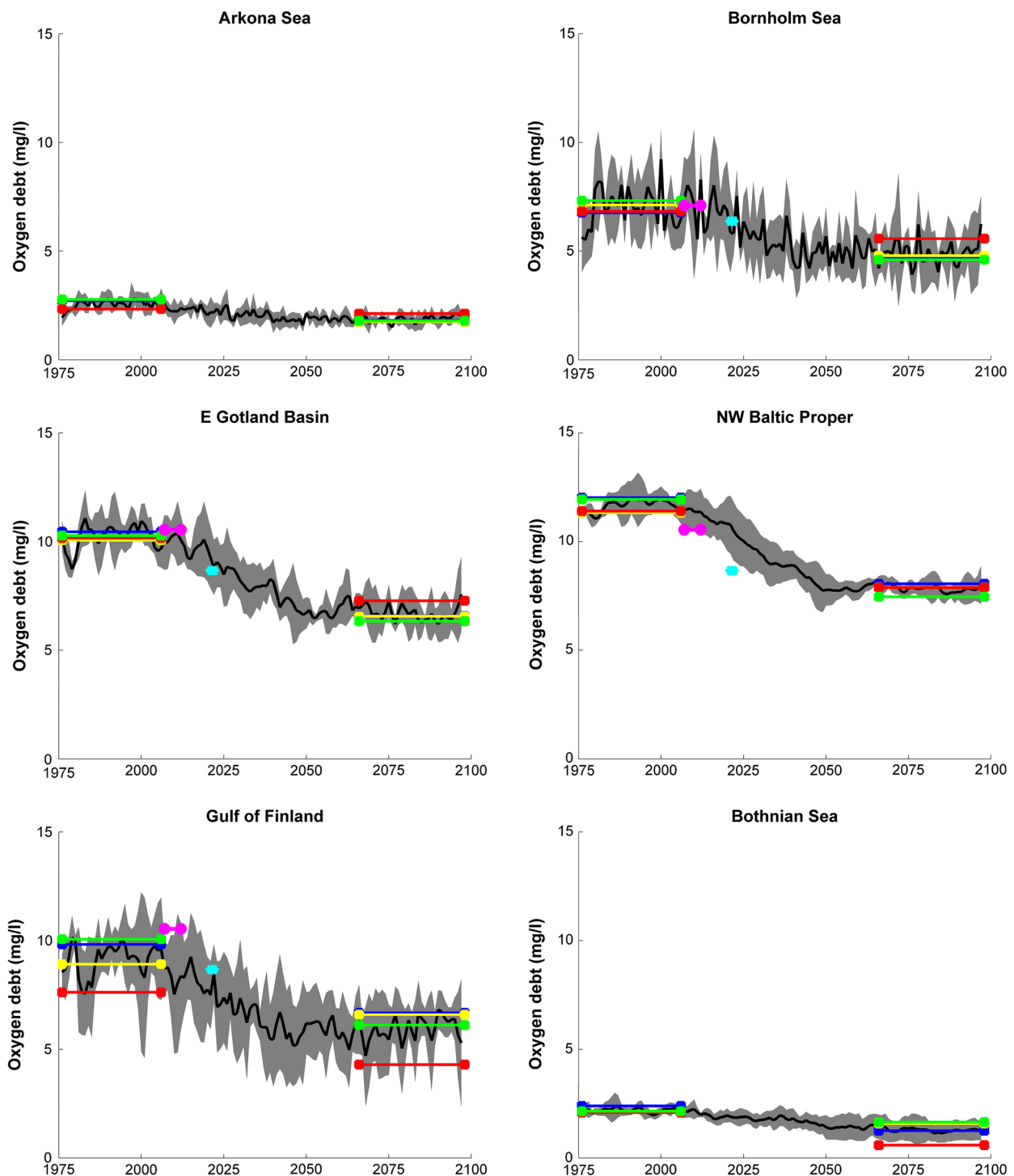
Fig. 2 Ensemble mean, annual average Secchi depth (in m) for 1976–2097 for selected sub-basins (black line) for BSAP and RCP 4.5. The gray shaded area denotes the range of ± 1 SD among the four ensemble members. The colored lines with solid squares at the beginning and end of the records are the averages for each climate simulation for the periods 1976–2005 and 2068–2097 (Model A—blue, Model B—yellow, Model C—red, Model D—green). The cyan dots are the HELCOM (2013b) thresholds for BSAP's Good Environmental Status (GES) shown in the year 2021 which is the year in which GES is supposed to be attained. The purple line with open circles is the mean (1997–2006) Secchi depth status from HELCOM (HELCOM 2013b; Table 4.3). The black line with the open circle is the median (1970–2000) Secchi depth from Savchuk et al. (2006; Table 3). The Savchuk values shown for the East Gotland Basin, the North-West Baltic Proper, Bornholm Basin, and Arkona Basin are those reported for the Baltic Proper. For further details see Table 1, but for annual average oxygen debt (in mg L^{-1}). The purple line with circles is the mean (2007–2011) oxygen debt status from HELCOM (2013b). For further details see Table 2

depend on the nutrient load scenario (i.e., increase under reference nutrient load conditions);

(3) an increase in the maximum duration of hypoxic periods in the western Baltic under reference nutrient conditions and no statistically significant changes under the BSAP, except for the Bornholm Basin; and

(4) an earlier occurrence of cyanobacteria blooms under both reference and BSAP scenarios in accordance with recent observations by Kahru and Elmgren (2014) who found approximately 20-day advancement during the period 1979–2013.

In this study, we further develop the analysis of changing extremes in future climate and focus on extreme occurrences of selected indicators with potential impact on Baltic Sea tourism such as 'tropical nights' defined as those days with a daily minimum 2 m air temperature > 20 °C (e.g., Fischer and Schär 2010), record-breaking SST events (e.g., Lehmann et al. 2015), and record-breaking number of days when cyanobacteria bloom are present.

DATA AND METHODS

Model Data

For the period 1975–2100, scenario simulations were performed using the RCO-SCOBI model, which consists of the physical Rossby Centre Ocean (RCO) model (Meier et al. 2003) and the Swedish Coastal and Ocean Biogeochemical (SCOBI) model (Eilola et al. 2009). The domain covers the Baltic Sea with open lateral boundary conditions in the northern Kattegat. RCO-SCOBI was forced by atmospheric surface fields from a Regional coupled atmosphere–ocean Climate Model (RCM) driven by lateral boundary data from four global General Circulation Models (GCMs). Runoff and nutrient loads were generated by a regional hydrological model forced by the same RCM data as RCO-SCOBI. The four GCMs were MPI-ESM-LR,[1] EC-EARTH,[2] IPSL-CM5A-MR[3], and Had-GEM2-ES,[4] henceforth called Models A to D. We applied two nutrient load scenarios, the BSAP scenario and a business-as-usual or reference scenario (REF). In the latter, socio-economic conditions were assumed to remain unchanged, but the nutrient loads slightly increase because of changing air temperature, precipitation, and terrestrial biogeochemical processes. For comparison, we also investigated a worst case scenario (WORST),

assuming increasing population with enhanced animal protein consumption, intensification of agricultural production, and no further nutrient load abatement strategies together with changing climate. Further, two greenhouse gas concentration scenarios corresponding to Representative Concentration Pathways (RCPs) 4.5 and 8.5 were studied (Moss et al. 2010). RCP 4.5 (mean scenario) and RCP 8.5 (high-end scenario) imply a radiative forcing at the end of the twenty-first century of 4.5 and 8.5 Wm^{-2}, respectively. For details of the model data from the scenario simulations, the reader is referred to Saraiva et al. (2019).

Estimation of oxygen debt in the open sea basins (HELCOM 2013b) in the model follows the method described by Carstensen et al. (2014). Oxygen debt was calculated for depths below a threshold defined from basin average salinity (S) profiles by the vertical grid point (S-point) where 68% of the change from surface to bottom salinity occurs (i.e., S-point $= 0.68 \times (S(\text{bottom}) - S(\text{surface})) + S(\text{surface})$; Bo Gustafsson, pers. comm.).

Analysis strategy

In a first step, model results during the historical period (1976–2005) were compared to observations. Simulated climatological mean profiles of temperature, salinity, oxygen, and nutrient concentrations at monitoring stations from model simulations driven by all four GCMs were compared to monitoring observations (Fig. S2). Further, the summer mean Secchi depth during May to October averaged for sub-basins (Fig. 1), the annual mean oxygen debt averaged for sub-basins (Fig. 2), the mean seasonal cycle of cyanobacteria concentrations at monitoring stations (S1 Evaluation of cyanobacteria concentration, Fig. S3), and the number of cyanobacteria bloom days during 2002–2008 (not shown) were evaluated.

In a second step, we analyzed projected changes between present (1976–2005) and future (2069–2098) climates. Changes in mean variables are mainly presented as electronic supplementary material. We analyzed atmospheric surface fields such as summer mean (July–August) 2 m air temperature (Fig. S4) and precipitation (Fig. S5), cloudiness and gustiness (not shown), seasonal mean SST (Fig. S6), annual mean sea surface and bottom salinity (Fig. S7), annual mean bottom oxygen concentrations (Fig. S8), winter (January–February) mean phosphate (Fig. S9) and nitrate (Fig. S10) concentrations, and annual mean phytoplankton concentrations (Fig. S11).

Further, ensemble mean changes in annual mean Secchi depth (Fig. 1) and oxygen debt below the halocline averaged for sub-basins (Fig. 2) were analyzed.
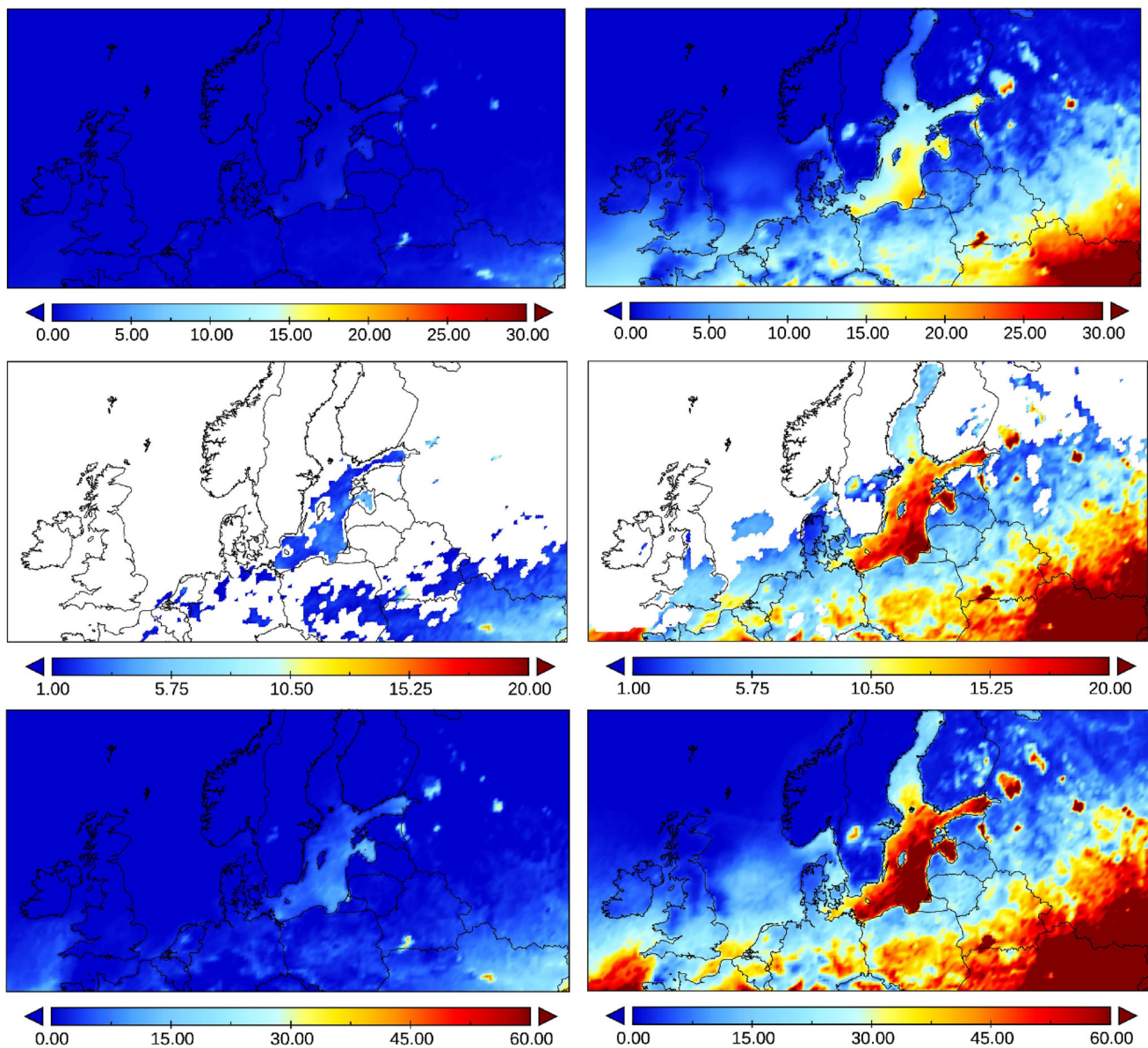
---

[1] https://www.mpimet.mpg.de.

[2] https://www.knmi.nl.

[3] http://icmc.ipsl.fr/.

[4] http://www.metoffice.gov.uk.

Fig. 3 Average annual number (upper panels), average annual number of consecutive days (middle panels), and maximum number of consecutive days (lower panels) of tropical nights (daily minimum > 20 °C) for 1970–1999 (left panels) and 2070–2099 (right panels). The ensemble mean under the RCP 8.5 scenario is shown

In a third step, we analyzed the changes in extremes such as tropical nights (Fig. 3), the number of summer (May to October) days with SST exceeding 18 °C, i.e., water conditions that will favor cyanobacteria blooms (Fig. S12), and record-breaking events in summer (June to August) mean SST (Fig. 4) and in the number of cyanobacteria bloom days (Fig. 5). A value is defined as record-breaking if it exceeds all previous values in the given time series. Looking at a single year in our model ensemble, we calculated the proportion of the ensemble members that generated a record-breaking event. This proportion can be called an 'observed' record-breaking probability. It can be higher or lower than

the expected value of $1/n$, in year n, in a random time series without a trend.

To check whether the deviation between the observed and expected number of record-breaking events is significant, we produced 10 000 ensembles of random time series, each of the same size as the model ensemble. From these we derived confidence intervals that were used to detect significant excursions from the natural variability of record-breaking events.

The detailed analysis of record-breaking events follows Lehmann et al. (2015). As mentioned above, we first defined a record-breaking function, indicating whether the
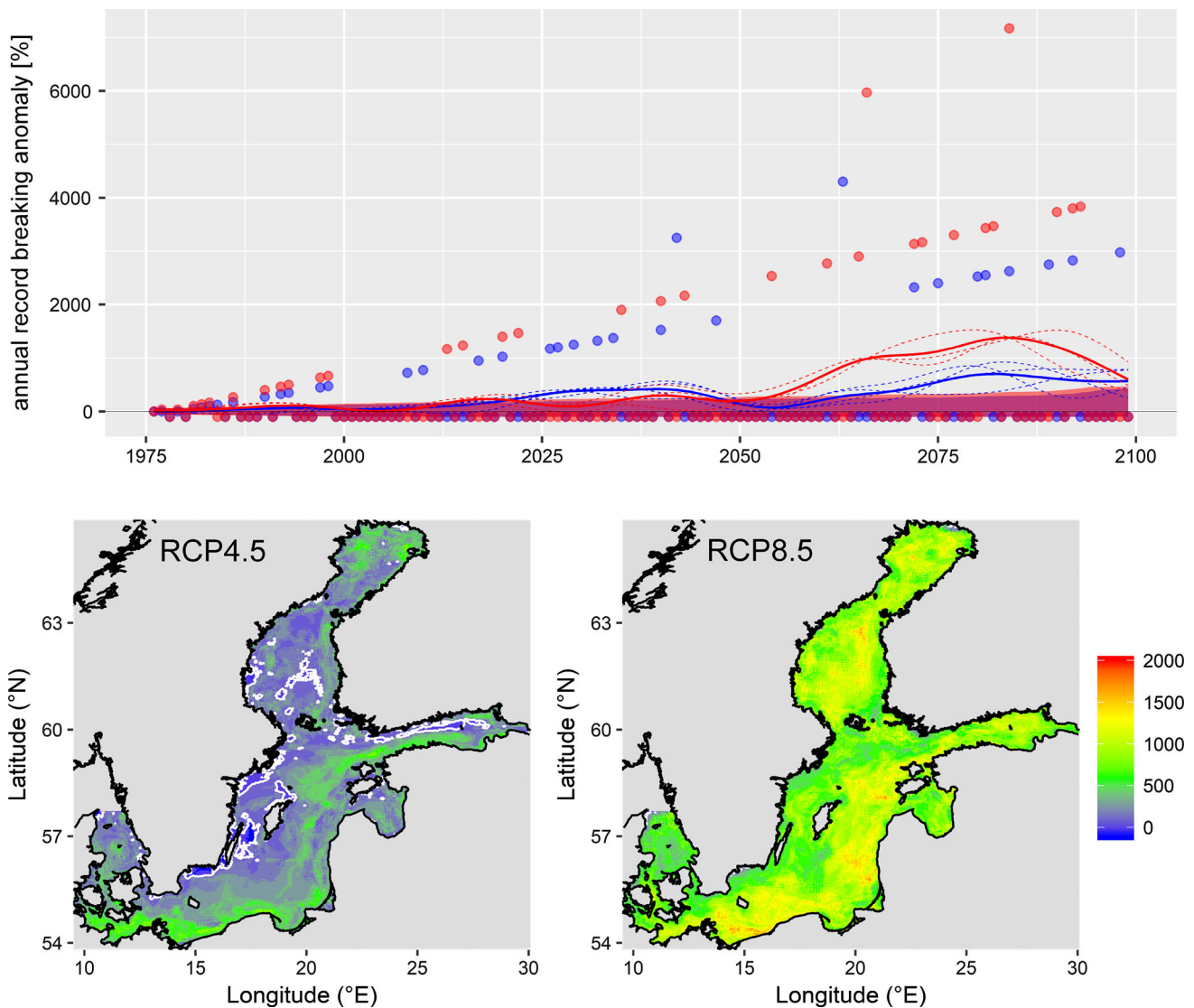
Fig. 4 Upper panel: Annual record-breaking anomaly R_{anom} of summer (June to August) mean sea surface temperature (SST) at Warnemünde (located in northeastern Germany at the Baltic Sea coast) (dots). The ensemble means of 4 (3) ensemble members during 1975–2098 under the emission scenarios RCP 4.5 (blue) and RCP 8.5 (red) are shown. Solid curves denote the long-term non-linear trend in this record-breaking anomaly calculated with a Gaussian filter with a width of 15 years. The dashed curves are the same as the solid curve, but for ensembles with a reduced number of members, each of them omitting one ensemble member. The shaded area denotes the confidence interval for the long-term non-linear trend in record-breaking anomaly: 95% of all 4-(3)-member ensembles of independent and identically distributed (iid) time series have a long-term trend within this range. Lower panels: record-breaking summer mean SSTs, under RCP 4.5 (left) and RCP 8.5 (right), ensemble mean of R_{anom} during 2069–2098. The white line (visible only in the lower left panel) shows where R_{anom} exceeds the value of 95% of all comparable iid time series ensembles

present-year value is the highest since the beginning of the time series. That is, for each annual time series y_i, $i = 1,...,n$ the record-breaking function (r_i) is defined as $r_i = 1$ if $y_i > y_j$ for all $j < i$ and $r_i = 0$ otherwise. The next step was to check whether the number of record events observed was higher or lower than we would expect. For a series of independent and identically distributed (iid) random variables, the expected value of r_i is $r_{iid,i} = 1/i$. So we

defined a record-breaking anomaly as $R_{anom,i} = 100\% \times (r_i - r_{iid,i})/r_{iid,i}$, indicating the extent to which the actual occurrence of record events exceeds the expected record probability. For a single time series, this function can only take two values at each data point, which are $(i - 1) \times 100\%$ (if this data point is a record value) or -100% (if it is not), but for an ensemble of time series, it makes sense to average R_{anom} across the ensemble members. In this case,
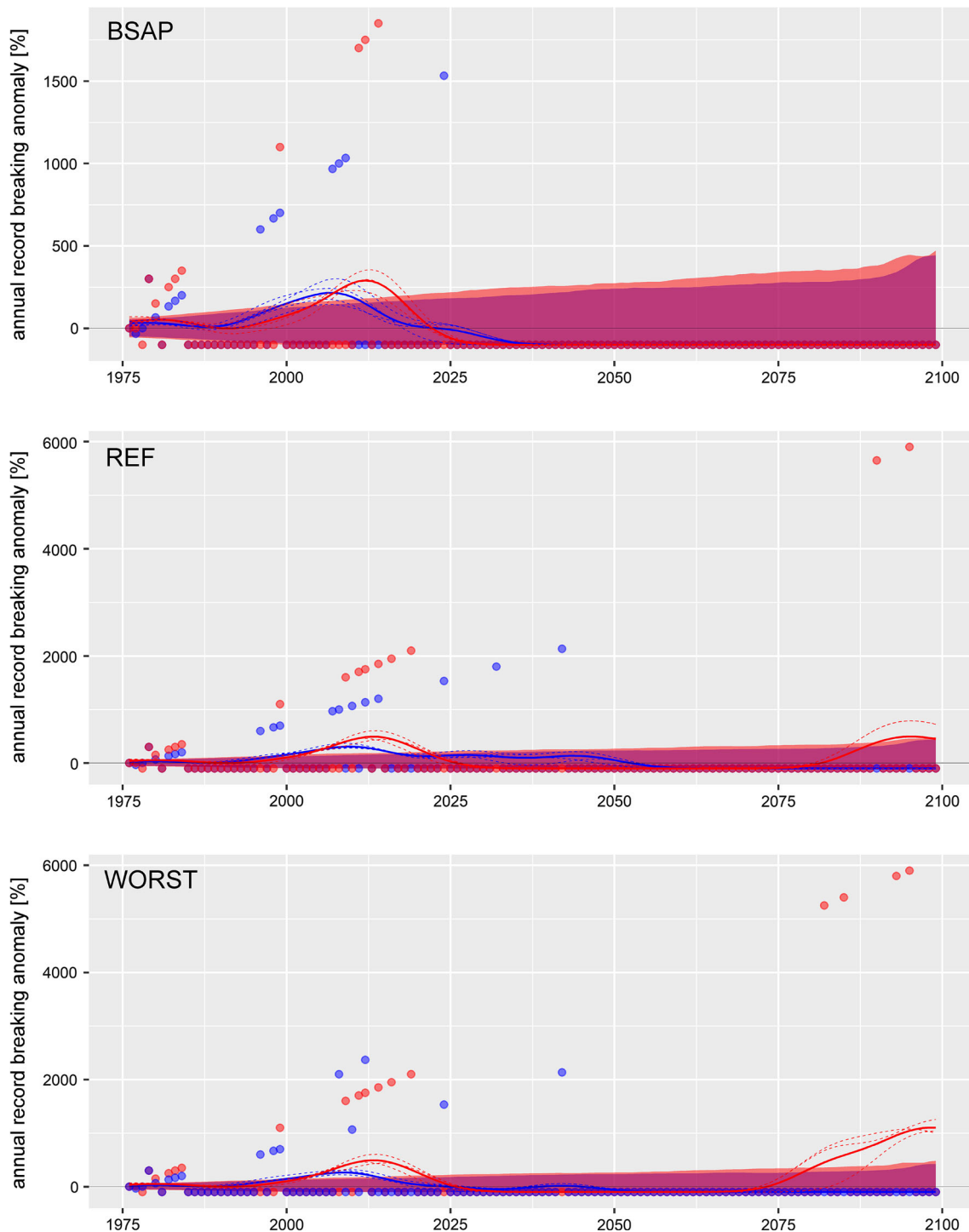
Fig. 5 Same as Fig. 4 (upper panel) but showing the number of cyanobacteria bloom days per summer averaged for the Baltic Sea. Blue: RCP 4.5. Red: RCP 8.5. Top panel: under the BSAP scenario. Middle panel: under the reference load scenario (REF). Bottom panel: under the worst case scenario (WORST)

the analysis tells us how much more frequently record values occur in this ensemble relative to their expected occurrence in an iid time series.

To explain the concept of record-breaking anomalies, we present an example. In year 5 of the time series in Fig. 4, the probability that this year is the hottest year since the beginning of the analysis timeframe should be $1/5 = 20\%$

without climate change. In our model ensemble (4 models), two of them (=50%) have a record-high event in year 5. The difference is +30%, which is +1.5 times the original probability. So our record-breaking anomaly is +150%. Our ensemble says that the probability of having a record-high event is 150% higher than without climate change.

A long-term trend in R_{anom} was extracted from the ensemble-averaged annual R_{anom} signal by applying a Gaussian filter with a width of 15 years. To check the sensitivity of the results to the presence or absence of individual ensemble members, we calculated the same long-term trend from a set of reduced ensembles, each of them omitting one single ensemble member.

To check whether the observed R_{anom} was significantly above or below zero, we calculated a confidence interval via a bootstrapping method. To do so, we generated 10 000 ensembles of random iid time series, with the same ensemble size as the original dataset. For each of these ensembles j, we calculated a long-term trend $R_{anom}^{(j)}$ as described above. The confidence interval outside which we regarded R_{anom} to be significantly different from zero was then defined by the 2.5 and 97.5 percentiles of $R_{anom}^{(j)}$.

In all figures, the ensemble mean calculated from the four downscaled GCMs is shown. The domains of the sub-basins follow Eilola et al. (2014), their Fig. 1.

RESULTS

Model evaluation

Temperature, salinity, oxygen, and nutrient concentrations

In all four climate simulations, the mean profiles of temperature, salinity, oxygen, and nutrient concentrations during the historical period compare well with monitoring data (Fig. S1). An exception is the nitrate concentration at BY31 (Landsort Deep). In all four simulations, nitrate concentration below the halocline is considerably underestimated probably because the stratification is too high and the oxygen concentration too low (Fig. S1), resulting in excessive prediction of denitrification. The reason why the ventilation of the deep water at BY31 is underestimated is unknown. However, the deep area around BY31 is small compared to the area of the entire Baltic with a mean depth of 52 m and the impact of the model's bias on biogeochemical cycles is very likely limited.

Secchi depth

The climatological mean simulated Secchi depth during the historical period is slightly underestimated in the Arkona

Basin and Bornholm Basin, and slightly overestimated in the North-West Baltic Proper and in the Gulf of Finland (Fig. 1, Table 1). However, the two data sets used for the evaluation (Savchuk et al. 2006; HELCOM 2013b) also differ considerably because the data were collected during different periods indicating considerable temporal variability (Fleming-Lehtinen and Laamanen 2012).

Oxygen debt

The climatological mean simulated oxygen debt is well simulated, but slightly overestimates (underestimates) in the North-West Baltic Proper (Gulf of Finland) the assessed status for 2007–2011 by HELCOM (2013b) (Fig. 2, Table 2).

Cyanobacteria

For a more detailed evaluation of the simulated cyanobacteria concentration, the reader is referred to Electronic supplementary material S1. In summary, the seasonal cycle of cyanobacteria blooms is well simulated but shifted seasonally. The model has some predictive capacity to reproduce the interannual variability and spatial distributions of blooms on the scale of sub-basins, but fails to predict the exact location of the blooms within the sub-basins (Meier et al. 2011b).

Changes in mean variables

Atmospheric variables

According to the RCP 8.5 ensemble mean, in the high-summer season (July to August), the near surface air temperature (SAT) in the Baltic Sea region will increase by 3 to 4 °C at the end of the century (2069 to 2098) compared to 1976–2005 (Fig. S4). The Baltic Sea itself exerts a moderating influence on the SAT rise. SAT increases more towards the east where continental climate dominates, and more towards the north where Arctic amplification is expected to have a positive feedback on climate change (Pithan and Mauritsen 2014). SATs in the Skagerrak and Kattegat area are projected to be warmer by 2 to 3 °C. Under the RCP 4.5 scenario, SAT around the Baltic Sea increases by about 2 °C.

According to the RCP 8.5 ensemble mean, for the high-summer season, precipitation at the end of the century reduces significantly in the western and southern Baltic Sea, including Skagerrak and Kattegat (Fig. S5). The Scandinavian Mountains, a mountain range running through the Scandinavian Peninsula from southern to northern Norway touching Sweden and northwestern-most Finland, and the northern part of Finland are projected to

receive more rain than during the reference period (1976–2005). In the pre-summer (May to June) and post-summer (September to October) seasons precipitation increases, although the changes are statistically significant only in the pre-summer season. The strongest increase is projected for the Scandinavian Mountains, in Finland and the southern Baltic Sea along the coasts of Poland, Lithuania, Latvia, and Estonia. The same pattern is observed for the ensemble mean of the RCP 4.5 scenario, although the changes are smaller (not shown).

In the high-summer season, gustiness of the near surface wind in the western and southern Baltic Sea and the Skagerrak and Kattegat is significantly reduced (not shown). Cloudiness does not change significantly.

Temperature, salinity, oxygen, nutrients, phytoplankton

Following the changes in SAT, the SSTs in the projections are also rising (Fig. S6). The SST increase in the summer season in the Baltic Proper is up to 3.5 °C under the RCP 8.5 scenario, and up to 2 °C under the RCP 4.5 scenario. In the pre-summer season, the Bothnian Sea is warming up much more than the rest of the Baltic Sea due to the earlier retreat of sea ice in that region. The coastal areas of Finland in the Bothnian Sea and the Gulf of Finland, and the south and east coast of Sweden in the Baltic Proper tend to warm up less than the average (Fig. S6).

The sea surface and bottom salinities are projected to decrease due to increased river runoff (Fig. S7). As the nutrient loads decrease both in the BSAP and REF scenarios, bottom oxygen concentrations increase except in simulations under RCP 8.5 and the REF scenario in combination (Fig. S11). In the latter situation, the changes in bottom oxygen concentrations are small because the increasing water temperature compensates for the effect of the reduced loads. The winter (January and February) mean phosphate concentrations averaged for the upper 10 m decrease slightly (Fig. S9). For nitrate concentrations, simulations projected an increase in the northern Baltic Sea (particularly in the Bothnian Sea and Bothnian Bay) and a decrease in the southern Baltic Sea (in the Baltic Proper or southern Baltic Proper except in regions influenced by runoff from the rivers Odra and Vistula under the REF scenario) (Fig. S10). Annual mean phytoplankton concentrations averaged for the upper 10 m are projected to decrease except in the simulations under RCP 8.5 and the REF scenario in combination (Fig. S11).

Secchi depth

In the combined RCP 4.5 and BSAP scenario, the annual mean Secchi depth is projected to increase in all sub-basins (Fig. 1). Larger changes are projected in today's eutrophic

sub-basins of the Baltic Proper. In the East Gotland Basin and in the Bothnian Sea, simulations suggested that GES (Tab. 1, HELCOM 2013b) will not be reached before the end of the century. According to our model ensemble, GES will only be achieved by 2021 in the Arkona Basin. However, the model shows systematic biases during the historical period, and relative changes might therefore be better indicators through which to examine progress towards GES.

Oxygen debt

In the combined RCP 4.5 and BSAP scenario, the annual mean oxygen debt below the halocline decreases in all sub-basins (Fig. 2). During the coming decade, simulations projected that GES will be reached in all sub-basins. For the North-West Baltic Proper only, the target oxygen debt is first achieved by 2040–2050, depending on the particular climate projection.

Cyanobacteria blooms

We found that the number of cyanobacteria bloom days per summer decreased considerably under the combined RCP 4.5 and BSAP scenario (not shown). A decrease (although smaller) was also found for the RCP 8.5 scenario.

Changes in extremes

Tropical nights

Under future climate, the number of tropical nights will significantly increase (Fig. 3). We found an increase in the average annual number, the average annual number of consecutive days with tropical nights, and the maximum number of consecutive days with tropical nights. In the model ensemble, the largest and smallest projected changes occurred in the southeastern and northwestern regions of the atmospheric model domain, respectively. It is of note that changes are more pronounced over the Baltic Sea than over the surrounding land. With an additional limitation to low wind speeds, the changes are more focused in the coastal zone (not shown). With global warming, the number of tropical nights increases more over the sea than over land because the larger heat content of the ocean compared to the land surface reduces not only the daily cycle but also the variability over the sea. Hence, the temperature over the sea remains high during the night, while temperature on land cools down faster. As the distribution of the daily minimum air temperature drops faster towards the extremes over the sea than over land, relatively more nights are warmer than the chosen threshold of 20 °C. Note that the future daily mean temperature in July and August in the

RCP 8.5 scenario is projected to be close to 20 °C (Fig. S4).

Water temperatures exceeding 18 °C

The number of days with SST exceeding 18 °C per summer increases in both RCP scenarios (Fig. S12). In the present climate, these days occur more frequently in the coastal zone than in the open sea region, particularly along the eastern and southern coasts. We project a mean increase of about 10–20 and 20–30 days under RCP 4.5 and RCP 8.5, respectively. The projected increase is larger over the open sea than over the coastal zone. The largest increase is projected for the eastern and southern Baltic Proper and the Gulf of Finland. The largest number of days with SST exceeding 18 °C per summer under future climate is also projected to occur along the eastern and southern coasts.

Record-breaking sea surface temperatures

The annual record-breaking anomaly in SST at Warnemünde (on the German coast) and its long-term trend are shown in Figs. 4 and S13). The model ensembles suggest that from 1975 until now, record temperatures were reached more frequently than would be expected from an iid time series without a long-term temperature trend ($R_{anom} > 0$). This increased frequency of record events is, however, not statistically significant. For the near future until 2050, the models show a significantly elevated probability of record temperatures (by about 400%) in the RCP 4.5 scenario. A less pronounced elevation of the probability of record temperatures (by about 200%) appears under the RCP 8.5 scenario, which is at the limit of statistical significance. The frequency in which new record-high temperatures occur at a specific location is influenced by the long-term trend of SST and random fluctuations. The latter might be even more important than the long-term trend. For example, during the first half of the twenty-first century the number of temperature records is more influenced by random variations than by the greenhouse gas emission scenario. This is also the case when the number of ensemble members is doubled (Fig. S13).

Under both climate scenarios, we then project a lack of record events around 2050, followed by a marked increase in the probability of record-breaking anomaly until 2099. So, in the second half of the twenty-first century, models run under the RCP 4.5 scenario project an eightfold increase in the probability that the present year will break the summer SST record since 1975 compared to the probability expected under a constant climate. Under the RCP 8.5 scenario, this probability will be increased 12-fold. These changes in the expected frequency of record SST occurrence are statistically significant.

Record-breaking summer mean SSTs increase more in the eastern than in the western Baltic Proper (Fig. 4). This pattern is similar to that projected for the mean number of summer days with SST exceeding 18 °C (Fig. S12) and is very likely to be caused by upwelling as the mean wind direction is from the southwest.

Record-breaking cyanobacteria blooms

Figure 5 shows the record-breaking anomaly for the number of days in a year on which a cyanobacterial bloom is projected to take place, that is, when the threshold concentration of 4 mg m^{-3} chlorophyll-*a* was exceeded by the cyanobacteria functional group in the model. This number of bloom days was averaged over the whole model domain, even if these blooms were only projected to occur in the central Baltic Sea and in the Gulf of Finland.

The long-term non-linear trend in the record-breaking anomaly shows a maximum in the recent past (around 2010) and a sharp decline afterwards. The maximum indicates a significant three- to fivefold enhancement in the record probability for the longest bloom duration. The decline thereafter can be considered a result of the lower phosphate loads to the Baltic Sea after the 1980s, which lead to lower phosphate concentrations and improved oxygen conditions in the bottom water after a time lag induced by phosphate retention in the Baltic Sea. This implies smaller blooms in the following period, which is evident in the absence of record blooms under all climate and nutrient load scenarios, leading to a record-breaking anomaly of less than zero. Precisely when record-duration blooms are projected to stop depends on the climate and nutrient load scenario applied in our model. In the case where the BSAP is implemented, our models suggest that record blooms will stop after 2025. Under the other nutrient load scenarios, our models suggest that record blooms may continue through the first half of the twenty-first century, although only under the RCP 4.5 scenario. If the BSAP is not implemented, the models suggest that under the RCP 8.5 scenario, record bloom events may reappear towards the end of the century, probably due to the strongly increased temperatures. None of these results depend on the presence or absence of individual ensemble members, except for the continuation of record blooms after 2025 under the RCP 4.5 scenario, as the dashed lines in Fig. 5 show.

DISCUSSION

We found considerable increases in the projections of (1) the number of tropical nights, the number of consecutive days with tropical nights, and the maximum number of

consecutive days of tropical nights, (2) the number of summer days with SST exceeding 18 °C, and (3) the record-breaking anomaly of summer mean SSTs. Overall, the changes in extremes follow the trends in the mean SAT and SST. However, we found a pronounced variability on time scales > 30 years in the record-breaking anomaly of summer mean SSTs. This suggests that despite global warming there might be several decades in the future without record-breaking events.

Our model ensembles also show an elevated number of record-breaking events in the present climate. This positive anomaly of record-breaking probabilities in the models cannot, however, be attributed to changing climate, since similar accumulations of record events may also occur in ensembles of iid time series, if they have as few members as our model ensembles. This means that the present-day positive record-breaking anomaly in our model experiment is not statistically significant. These findings highlight the need for better understanding of the variability surrounding extremes.

Further, we showed that the larger heat content of the Baltic Sea, in comparison to the land surface, plays an important role in the evolution of some extremes such as tropical nights. These changes in extremes could have important consequences for the Baltic Sea ecosystem and also for the anthroposphere. Both human health and tourism are very likely to be affected by changes in temperature extremes (citations to research on human health, e.g., Patz et al. 2005; Kenney et al. 2014; and tourism, e.g., Bigano et al. 2005, 2006; UNWTO and UNEP 2008; Scott et al. 2012).

The record-breaking anomaly in the number of cyanobacteria bloom days per summer is projected to decline under all considered nutrient load scenarios as a consequence of the decreasing sea surface phosphate concentration. However, if the BSAP is not implemented, record-breaking cyanobacteria bloom events may reappear at the end of the century under the RCP 8.5 scenario because of the high level of warming, in particular due to the increased number of summer days with SST exceeding 18 °C that favor cyanobacteria growth. An additional impact might also be expected from the significantly reduced high-summer seasonal gustiness of the near surface wind in the western and southern Baltic Sea and the Skagerrak and Kattegat because cyanobacteria preferably to grow under warm water and low wind speed conditions. In addition, clear skies with enhanced radiation favor cyanobacteria blooms. As cloudiness does not change in our ensemble of climate simulations, the latter driver does not play a significant role here. As in all models, the predictive capacity of the model regarding the spatial extent of cyanobacteria blooms is still limited, because detailed impacts on local conditions such in the coastal zone cannot be calculated.

Nevertheless, the occurrence of cyanobacteria blooms is perhaps the most important aspect of human perception of eutrophication in the Baltic Sea. Hence, record-breaking events will influence tourism and other human activities. In this study, we made a first attempt to address changing extremes of societal relevance, and showed that the concept of record-breaking events can be useful and informative, even for relatively small ensembles of regional climate projections because the results do not change when we remove one of the four ensemble members from the analysis.

Our results suggest that record-breaking incidences of cyanobacteria blooms will likely cease in the relatively near future which might be beneficial for human health and tourism in the region. By contrast, record-breaking incidences of tropical nights and elevated temperatures (heat waves) will likely increase, which might be detrimental for human health. Studies on the relative impacts of reduced incidence of blooms vs increased temperatures on both health and tourism do not exist for the Baltic Sea region. However, Kenney et al. (2014) found that extreme heat events, characterized by consecutive summer days of high maximum and minimum daily temperatures, are the most prominent cause of weather-related human mortality in the U.S., responsible for more deaths than flooding, lightning, hurricanes, tornados, and earthquake combined. Further, climate warming will increase the number of Vibrio-caused infections and incidences of Lyme disease (Kenney et al. 2014). Hence, we speculate that at the end of the century the impact of increased incidences of temperature extremes on human health will dominate all pressures on society.

CONCLUSIONS

The main conclusions of this study are as follows:

1. Assuming perfect implementation of the BSAP, in most of Baltic sub-basins the baseline values of GES will be reached for the Secchi depth and oxygen debt indicators under the RCP 4.5 scenario during the twenty-first century. However, in some sub-basins GES will not be realized in 2021 as planned, but considerably later in the second half of this century.
2. The projected increase in temperature extremes shows non-linear changes that differ from the changes projected for the temperature means. For instance, tropical nights increase more over the open sea than over the surrounding land, highlighting the important role of the Baltic Sea for regional climate.

3. A pronounced variability over time scales > 30 years is found in the record-breaking anomaly of summer mean SSTs, suggesting that there might be decades in the near future without record-breaking events.

4. If the BSAP is implemented successfully, our models suggest that record-breaking cyanobacteria blooms will not occur in the Baltic Sea in the future. Under the REF and WORST nutrient scenarios, record-breaking cyanobacteria blooms may, however, reappear at the end of the century.

REFERENCES

Bigano, A., A. Goria, J. Hamilton, and R.S.J. Tol. 2005. The Effect of Climate Change and Extreme Weather Events on Tourism. Report. https://papers.ssrn.com/sol3/papers.cfm?abstract_id=673453.

Bigano, A., J.M. Hamilton, and R.S.J. Tol. 2006. The impact of climate on holiday destination Choice. *Climatic Change* 76: 389. https://doi.org/10.1007/s10584-005-9015-0.

Carstensen, J., J.H. Andersen, B.G. Gustafsson, and D.J. Conley. 2014. Deoxygenation of the Baltic Sea during the last century. *Proceedings of the National Academy of Sciences of the United States of America* 111: 5628–5633. https://doi.org/10.1073/pnas.1323156111.

Eilola, K., H.E.M. Meier, and E. Almroth. 2009. On the dynamics of oxygen, phosphorus and cyanobacteria in the Baltic Sea: A model study. *Journal of Marine Systems* 75: 163–184. https://doi.org/10.1016/j.jmarsys.2008.08.009.

Eilola, K., E. Almroth-Rosell, and H.E.M. Meier. 2014. Impact of saltwater inflows on phosphorus cycling and eutrophication in the Baltic Sea: A 3D model study. *Tellus A* 66: 23985. https://doi.org/10.3402/tellusa.v66.23985.

Fischer, E.M., and C. Schär. 2010. Consistent geographical patterns of changes in high-impact European heatwaves. *Nature Geoscience* 3: 398.

Fleming-Lehtinen, V., and M. Laamanen. 2012. Long-term changes in Secchi depth and the role of phytoplankton in explaining light attenuation in the Baltic Sea. *Estuarine, Coastal and Shelf Science* 102: 1–10.

HELCOM. 2013a. Copenhagen Ministerial Declaration, HELCOM Ministerial Meeting, Copenhagen, Denmark.

HELCOM. 2013b. Approaches and methods for eutrophication target setting in the Baltic Sea region. Baltic Sea Environment Proceedings 133.

HELCOM. 2018. State of the Baltic Sea – Second HELCOM holistic assessment 2011–2016. Baltic Sea Environment Proceedings 155. ISSN 0357-2994. http://www.helcom.fi/baltic-sea-trends/holistic-assessments/state-of-the-baltic-sea-2018/reports-and-materials/.

Kahru, M., and R. Elmgren. 2014. Multidecadal time series of satellite-detected accumulations of cyanobacteria in the Baltic Sea. *Biogeosciences* 11: 3619–3633. https://doi.org/10.5194/bg-11-3619-2014.

Kenney, M.A., A.C. Janetos, et al. 2014. National Climate Indicators System Report. National Climate Assessment and Development Advisory Committee.

Lehmann, J., D. Coumou, and K. Frieler. 2015. Increased record-breaking precipitation events under global warming. *Climatic Change* 132: 501. https://doi.org/10.1007/s10584-015-1434-y.

Meier, H.E.M., R. Döscher, and T. Faxén. 2003. A multiprocessor coupled ice-ocean model for the Baltic Sea: Application to salt inflow. *Journal of Geophysical Research* 108: 3273. https://doi.org/10.1029/2000JC000521.

Meier, H.E.M., H.C. Andersson, K. Eilola, B.G. Gustafsson, I. Kuznetsov, B. Müller-Karulis, T. Neumann, and O.P. Savchuk. 2011a. Hypoxia in future climates: A model ensemble study for the Baltic Sea. *Geophysical Research Letters* 38: L24608. https://doi.org/10.1029/2011GL049929.

Meier, H.E.M., K. Eilola, and E. Almroth. 2011b. Climate-related changes in marine ecosystems simulated with a three-dimensional coupled biogeochemical-physical model of the Baltic Sea. *Climate Research* 48: 31–55.

Meier, H.E.M., K. Eilola, E. Almroth-Rosell, S. Schimanke, M. Kniebusch, A. Höglund, P. Pemberton, Y. Liu, et al. 2019a. Disentangling the impact of nutrient load and climate changes on Baltic Sea hypoxia and eutrophication since 1850. *Climate Dynamics* 53: 1145–1166. https://doi.org/10.1007/s00382-018-4296-y.

Meier, H.E.M., K. Eilola, E. Almroth-Rosell, S. Schimanke, M. Kniebusch, A. Höglund, P. Pemberton, Y. Liu, et al. 2019b. Correction to: Disentangling the impact of nutrient load and climate changes on Baltic Sea hypoxia and eutrophication since 1850. *Climate Dynamics* 53: 1167–1169. https://doi.org/10.1007/s00382-018-4483-x.

Moss, R.H., J.A. Edmonds, K.A. Hibbard, M.R. Manning, S.K. Rose, D.P. Van Vuuren, T.R. Carter, S. Emori, et al. 2010. The next generation of scenarios for climate change research and assessment. *Nature* 463: 747–756.

Neumann, T., K. Eilola, B. Gustafsson, B. Müller-Karulis, I. Kuznetsov, H.E.M. Meier, and O.P. Savchuk. 2012. Extremes of temperature, oxygen and blooms in the Baltic Sea in a changing climate. *Ambio* 41: 574–585. https://doi.org/10.1007/s13280-012-0321-2.

Patz, J.A., D. Campbell-Lendrum, T. Holloway, and J.A. Foley. 2005. Impact of regional climate change on human health. *Nature* 438: 310–317.

Pithan, F., and T. Mauritsen. 2014. Arctic amplification dominated by temperature feedbacks in contemporary climate models. *Nature Geoscience* 7: 181.

Rabalais, N.N., R.J. Díaz, L.A. Levin, R.E. Turner, D. Gilbert, and J. Zhang. 2010. Dynamics and distribution of natural and human-caused hypoxia. *Biogeosciences* 7: 585–619. https://doi.org/10.5194/bg-7-585-2010.

Saraiva, S., H.E.M. Meier, H. Andersson, A. Höglund, C. Dieterich, M. Gröger, R. Hordoir, and K. Eilola. 2019. Uncertainties in projections of the Baltic Sea ecosystem driven by an ensemble of

global climate models. *Frontiers in Earth Science* 6: 244. https://doi.org/10.3389/feart.2018.00244.

Savchuk, O.P., U. Larsson, L. Elmgren, and M. Rodriguez Medina. 2006. Secchi depth and nutrient concentration in the Baltic Sea: model regressions for MARE's Nest. Department of Systems Ecology, Stockholm University. Technical Report. Stockholm, Sweden.

Scott, D., S. Gössling, and C.M. Hall. 2012. International tourism and climate change. *WIREs Climate Change* 3: 213–232. https://doi.org/10.1002/wcc.165.

Sherman, K., M. Sissenwine, V. Christensen, A. Duda, G. Hempel, C. Ibe, S. Levin, D. Lluch-Belda, et al. 2005. A global movement toward an ecosystem approach to management of marine resources. *Marine Ecology Progress Series* 300: 275–279.

UNWTO and UNEP. 2008. Climate Change and Tourism – Responding to Global Challenges. World Tourism Organization and the United Nations Environment Programme, Madrid, Spain. ISBN: 978-92-844-1234-1 (UNWTO), ISBN: 978-92-807-2886-6 (UNEP). https://sdt.unwto.org/sites/all/files/docpdf/climate2008.pdf.

AUTHOR BIOGRAPHIES

H. E. Markus Meier (✉) is a professor in Physical Oceanography and head of the Department of Physical Oceanography and Instrumentation at the Leibniz Institute for Baltic Sea Research Warnemünde. He is also senior scientist at the Research Department of the Swedish Meteorological and Hydrological Institute. His research interests include the understanding of climate dynamics and climate change on global and regional scales, detection, and attribution and coupled physical-biogeochemical modeling in particular of the Baltic Sea.
Address: Department of Physical Oceanography and Instrumentation, Leibniz Institute for Baltic Sea Research Warnemünde, 18119 Rostock, Germany.
Address: Department of Research and Development, Swedish Meteorological and Hydrological Institute, 60 176 Norrköping, Sweden.
e-mail: markus.meier@io-warnemuende.de

Christian Dieterich is a scientist at the Research Department of the Swedish Meteorological and Hydrological Institute. He works on coupled regional modeling of the Baltic Sea region including regional climate changes scenarios and on sea-level changes for the Baltic Sea.
Address: Department of Research and Development, Swedish Meteorological and Hydrological Institute, 60 176 Norrköping, Sweden.
e-mail: christian.dieterich@smhi.se

Kari Eilola is senior scientist and research leader of the marine environmental research group at the oceanographic research unit at SMHI. His research interests focus on oceanography and physical-biogeochemical modeling of the Baltic Sea.
Address: Swedish Meteorological and Hydrological Institute, 42 671 Västra Frölunda, Sweden.
e-mail: kari.eilola@smhi.se

Matthias Gröger is a scientist at the Research Department of the Swedish Meteorological and Hydrological Institute. He works on coupled regional modeling of the Baltic Sea region including regional climate changes scenarios and on sea-level changes for the Baltic Sea.
Address: Department of Research and Development, Swedish Meteorological and Hydrological Institute, 60 176 Norrköping, Sweden.
e-mail: matthias.groger@smhi.se

Anders Höglund is a scientist at the Research Department of the Swedish Meteorological and Hydrological Institute. He is a mathematician and his research areas include oil spill modeling and current patterns.
Address: Department of Research and Development, Swedish Meteorological and Hydrological Institute, 60 176 Norrköping, Sweden.
e-mail: anders.hoglund@smhi.se

Hagen Radtke is a postdoctoral researcher at the Department of Physical Oceanography and Instrumentation at the Leibniz Institute for Baltic Sea Research Warnemünde. His research focuses on understanding the Baltic Sea system with the aid of numerical models, from process to climate scales.
Address: Department of Physical Oceanography and Instrumentation, Leibniz Institute for Baltic Sea Research Warnemünde, 18119 Rostock, Germany.
e-mail: hagen.radtke@io-warnemuende.de

Sofia Saraiva is a postdoctoral researcher at the University of Lisbon, IST, MARETEC. Her research interests focus on the link between the different processes in the marine environment (physical, biogeochemical, and ecological) using and developing numerical modeling tools, namely coupled physical-biogeochemical models.
Address: Environment and Energy Section, Department of Mechanical Engineering, Instituto Superior Técnico, Technical University of Lisbon, 1049-001 Lisbon, Portugal.
e-mail: sofia.maretec@tecnico.ulisboa.pt

Iréne Wåhlström is a scientist at the Research Department of the Swedish Meteorological and Hydrological Institute. She is a marine chemist with her research interest in biogeochemistry in the Baltic Sea and the Arctic Ocean, with the focus on the carbonate system and methane.
Address: Department of Research and Development, Swedish Meteorological and Hydrological Institute, 60 176 Norrköping, Sweden.
e-mail: irene.wahlstrom@smhi.se